A formation scenario for faint and ultra-faint dwarf spheroidal galaxies

C.A. Aravena[1], M. Fellhauer[1], F. Urrutia Zapata[1] & A.G Alarcón Jara[1]

[1] *Departamento de Astronomía, Universidad de Concepción, Chile*

Contact / cataaravena@udec.cl

Resumen / Las galaxias enanas esferoidales débiles y ultradébiles representan una nueva población de galaxias enanas esferoidales clásicas, con propiedades físicas muy similares. Corresponden a los sistemas del Universo local más dominados por materia oscura, con magnitudes absolutas entre $-7 < \mathrm{M_v} < -1.5$, masa estelar del orden de $10^2\mathrm{M}_\odot < \mathrm{M}_\star < 10^5\mathrm{M}_\odot$, además de ser las galaxias enanas con más baja metalicidad en el Grupo Local ($[\mathrm{Fe/H}] \lesssim -2.5$). Son extremadamente valiosas para el entendimiento de la formación de estructuras en el Universo y una importante prueba de la formación de galaxias a escalas más pequeñas. Desarrollamos simulaciones numéricas usando nuestros modelos de formación de galaxias enanas esferoidales clásicas previos, para estudiar un nuevo modelos de formación de galaxias enanas esferoidales débiles y ultradébiles con un potencial de fondo, que imita un halo de materia oscura. Las estrellas se encuentran inicialmente en equilibrio virial, distribuidas en una región de formación estelar filamentaria con una distribución fractal al interior de un halo analítico, formando el componente luminoso que hoy observamos. Seguimos su evolución por un periodo de 5 000 millones de años.

Abstract / Faint and ultra-faint dwarf spheroidal galaxies represent a new population of dwarf spheroidal galaxies with very similar physical properties. They are the most dark matter dominated systems in the local Universe with absolute magnitudes between $-7 < \mathrm{M_v} < -1.5$, a stellar mass range of $10^2\mathrm{M}_\odot < \mathrm{M}_\star < 10^5\mathrm{M}_\odot$ and they are the most metal-poor ($[\mathrm{Fe/H}] \lesssim -2.5$) dwarfs in the Local Group. They are extremely valuable for our understanding of structure formation in the Universe and useful probes of galaxy formation on smallest scales. We perform numerical simulations using our previous formation models of classical dwarf spheroidal galaxies to study a star formation scenario for faint and ultra-faint dwarf spheroidal galaxies with a strong background potential mimicking the dark matter halo. Our stars are initially in virial equilibrium and placed in a filamentary stellar distribution, a fractal distribution within an analytical halo, building the faint luminous components that we observe. We follow their evolution for 5 Gyr.

Keywords / methods: numerical — galaxies: dwarf — galaxies: formation — galaxies: star formation — galaxies: kinematics and dynamics

1. Introduction

The dwarf spheroidal galaxies (dSph) around the Milky Way offer a unique opportunity to investigate galaxy formation and evolution by studying the photometric properties of the resolved stellar populations (Okamoto et al., 2012). Since 2005, the Sloan Digital Sky Survey (SDSS) and similar surveys have discovered a large number of new dwarf galaxies orbiting around the Milky Way. A new population of dwarf galaxies in the Local Group (LG), known as ultra-faint dwarfs (UFDs), appears to be an extension of the classical dSphs with very similar physical properties.

UFDs galaxies do not contain any gas at the present time and their stars are very iron-poor, with ages $\gtrsim 10-12$ Gyr, so they are the most metal poor population in the LG, and maybe galaxies where star formation ended in the earliest epoch of the Universe (Tollerud et al., 2011; Vincenzo et al., 2014). These systems can have luminosities smaller than $\sim 1\,000$ $\mathrm{L}_\odot$, and are $\sim 10-1\,000$ times fainter that the classical dSph or even most of the Galactic globular clusters. They are the most dark matter (DM) dominated systems, do not show recent star formation activity and have a high mass-to-light ratio > 100.

They are located close to the Milky Way, mostly within its virial radius. They show different morphologies and most of the dwarfs are elongated, demonstrating that they are not spherically symmetric systems and probably do not have an isotropic velocity dispersion. Several dwarfs also appear irregular, opening up the possibility that their structure has been significantly affected by the tidal field of the Milky Way.

The origin of UFDs is a matter of ongoing debate. Several solutions have been suggested so far for resolving the crisis. It is common for galaxy formation models to alleviate the missing satellite problem by truncating the star formation in dark matter halos below some nominal mass threshold, sometimes termed the "filtering mass". With this threshold tuned to match the observations, there are several models that attempt to explain the origin of dSph galaxies by considering different mechanisms. Some of them are based on the tidal and ram-pressure stripping model (Mayer et al., 2007). The model proposed by D'Onghia et al. (2009) considers a mechanism known as resonant stripping and can be used to explain the formation of isolated dSph galaxies. There is another model that explains the formation of dwarf galaxies based on energy and momentum conservation when gas-rich galaxies interact, in which the dSph galaxies are in fact DM free tidal dwarf galaxies (Metz et al., 2007), and there are models which consider dwarf galaxies in isolation, but they usually take only a smooth gas distribution into account and focus on higher masses for the dwarfs (Assmann et al., 2013b; Alarcón Jara et al., 2018).

Models that explain the origin of dSph galaxies in isolation with high resolution are proposed by Assmann et al. (2013a). Their fiducial model tested a possible scenario for formation of dSph galaxies using the particle mesh code SUPERBOX, where they performed numerical simulations of isolated galaxies, but distributed the newly formed stars into dissolving star clusters (SCs) within the DM halo. The model is based on the assumption that the stars form in hierarchical structures, i.e. SCs. The star formation events range from slowly forming stars in small clusters and associations to intense starbursts, in gas-rich environments, typically producing a few hundred young SCs, within a region of just a few hundred parsec.

Assmann's models proposed that the dynamical evolution of these SCs, that is, their dissolution due to the gas expulsion, may explain the formation of classical dSph galaxies, including all their irregularities in the stellar kinematic distribution as well as surviving SCs around them. The SCs form with low star formation efficiency (SFE) and, thus, are designed to dissolve inside the DM halo to form luminous component of the dSph galaxy.

Alarcón Jara et al. (2018) present a dissolving SCs scenario adding different star formation histories (SFHs) to the models, as an extension of the work of Assmann et al. (2013a), placing SCs into the simulations at different moments in time. The SCs form with low SFE and thus, are designed to dissolve inside the DM halo to form the luminous component of the dSph galaxy.

Alarcón Jara et al. (2018) show this formation scenario works even with different SFHs, DM halo profiles and SFEs to dissolve the SCs. They not only reproduce the observational data that we have today, also provide observers with predictions for future observations.

We perform numerical simulations using the Astrophysical Multipurpose Software Environment (AMUSE), to study a star formation scenario for faint and ultra-faint dwarfs spheroidal galaxies based on the dissolving star clusters models. We study a formation scenario in which stars are initially placed in a fractal distribution inside the centre of the DM halo, building the faint luminous component that we observe.

2. Method and initial conditions

The stars are initially placed in a fractal distribution. We use the method introduced by Goodwin & Whitworth (2004) to generate a initial sub-structured distributions. This method defines a cube of size $N_{\rm div} = 2$ in which the fractal is created. Starting in the centre of the cube with a first-generation parent which is divided in $N^3_{\rm div}$ sub-cubes. Each sub-cube, called child can turn into a parent for the next generation with a probability of $N^{\rm D-3}_{\rm div}$, where D is the fractal distribution. Specifically for us, we choose a value of $N^3_{\rm div} = 8$ and a fractal dimension of $\rm D = 1.6$. An example of this is shown in (Fig. 1, top left panel). The process is repeated until the number of children reaches a larger number than the number of particles. The velocities of the children are inherent from the parents including a random component that decreases with each new generation (Domínguez et al., 2017; Goodwin & Whitworth, 2004).

For our simulations of Segue 1 we consider 700 particles in virial equilibrium with equal mass ($\rm M_\star = 0.5\ M_\odot$) i.e. a total luminous mass of $\rm M = 350\ M_\odot$. We assume a physical size $\rm r_{fractal}$ of the system of 10, 30 and 50 pc.

We consider an analytic background potential. For this set of simulations we use a Plummer potential (Plummer, 1911):

$$\rho(r) = \frac{3\rm M^3_{Pl}}{4\pi \rm R_{Pl}}\left(1+\frac{r^2}{\rm R^2_{Pl}}\right)^{-\frac{5}{2}} \qquad (1)$$

with $\rm M_{Pl}$ and $\rm R_{Pl}$ the Plummer mass and Plummer radius respectively. For Segue 1, we have an effective radius $\rm R_{eff} = 30$ pc and within that $\rm R_{eff}$ the measured mass in DM is $\rm M_{halo}(r_h) = 6 \times 10^5\ M_\odot$. Our DM halo has a default scale-length of $\rm R_{Pl} = 1$ kpc. To obtain the measured dynamical mass within $\rm r_h$ we choose a Plummer mass of $\rm M_{Pl} = 2.15 \times 10^{10}\ M_\odot$.

3. Results

We follow the evolution of the initial fractal distribution within an analytical halo for 5 Gyr. We choose three different values for $\rm r_{fractal}$, namely, 10, 30 and 50 pc and perform for each value three different random realisations.

In Fig. 1 we show an example of the initial conditions and the time evolution of our distribution of stars. The initial radius $\rm r_{fractal}$ in the shown example is 50 pc. We note that even after 5 Gyr of evolution, the galaxy is still evolving and we recognise that the distribution of stars form a luminous object that resembles an UFD galaxy.

Fig. 2 shows the time-evolution of the Lagrangian radii (10, 20,..., 90% of the total mass) for the same distribution of stars as shown in Fig. 1. We see that 5 Gyr are not enough for the Lagrangian radii to stay constant.

To determine the effective radius, we would have to fit single Sérsic profiles to our simulation data, but for the kind of distribution of stars we obtain after 5 Gyr of evolution (see Fig. 1) we have to consider the Lagrangian radii at 50 % of the total mass have to instead. In Fig. 3 we show the half-mass radius against the initial size of the fractal. As the scale-length of a dSph usually should be smaller than the half-mass radius, we see that for our choice of DM halo we need fractal distribution of 50 pc or more.

What is very clearly visible is, that our formation scenario produces objects that have the distorted shapes of UFD intrinsically, without the need of an external influence.

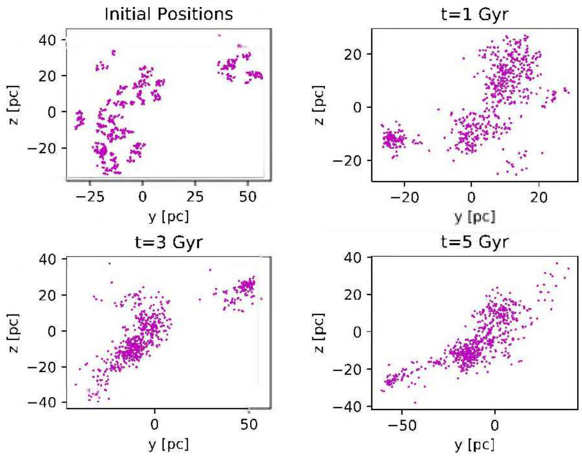

Figure 1: Example of the evolution of the distribution of stars from t=0 to t=5 Gyr. Top left panel: Initial distribution of stars at t=0 from a turbulent gas cloud for Segue I. The filamentary stellar formation region is form for 700 particles with equal mass i.e. a total luminous mass of M=350 $M_{\odot}$. The purple points represent the stars ($M_{\star}$=0.5 $M_{\odot}$) in virial equilibrium, with a fractal distribution of D = 1.6 in a radius of $r_{\rm fractal}$ = 50 pc. Top right: Distribution of stars after 1 Gyr of evolution. Bottom right: Distribution of stars after 3 Gyr of evolution. Bottom left: Final state of the distribution of stars after 5 Gyr.

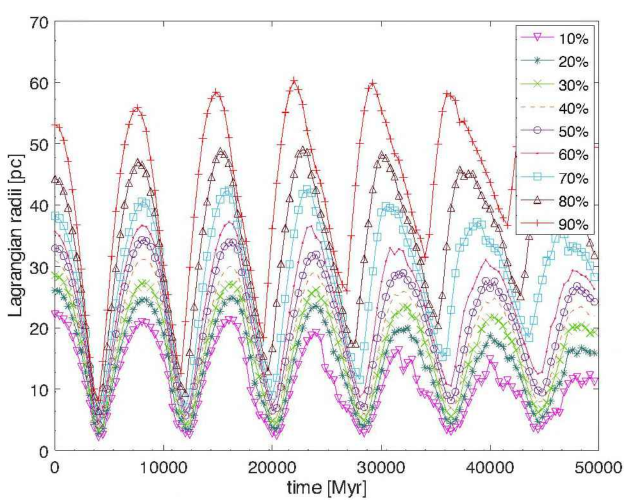

Figure 2: Lagrangian radii of our initial model with a fractal radius of $r_{\rm fractal}$ = 50 pc. The plot shows the Lagrangian radii between 10 % to 90 % of the total mass. We concluded that 5 Gyr are not enough for radii stay constant.

4. Conclusions

In this paper we tested a possible formation scenario, originally proposed by Assmann et al. (2013a,b) for the formation of UFD galaxies with numerical simulations using AMUSE and the direct N-body integrator ph4. In our simulations we considered the evolution of different fractal distributions of 700 particles within an analytical halo with a Plummer distribution. From the Lagrangian radii we observe that even after 5 Gyr of evolution the galaxy is still evolving (see Fig. 2).

We conclude that due to the initial fractal distributions the kind of distribution of stars we obtain after 5 Gyr of evolution is still complex to study the effective radius of the galaxy, so is necessary follow their evolution for the next 5 Gyr.

On the other hand, our results show that the variation in the fractal radius of the initial distributions of stars can produce, in some cases, results far away from the observational data that we have today, making necessary study the impact on the variation of the Plummer radius for the analytical halo as well.

Our main result is that our final object forms a luminous object that resembles a UFD galaxy like Segue 1, patchy distribution of stars observed ellipticities and effective radii velocity dispersion.

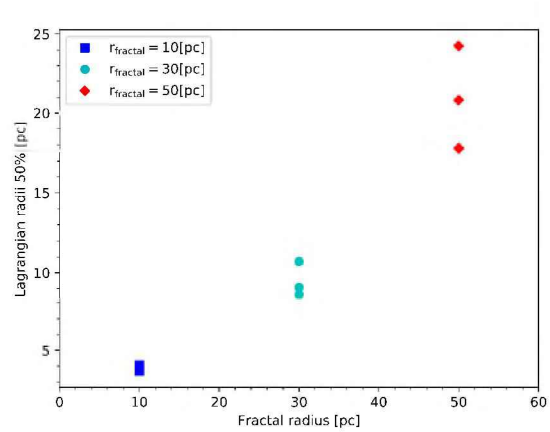

Figure 3: Lagrangian radii at 50 % after 5 Gyr of evolution as a function of the fractal radius of the distribution of stars. Blue squares represent the Lagrangian radii at 50 % as a function of their fractal radius of 10 pc. Cyan circles represent the relation between the Lagrangian radii at 50 % of the total mass with a fractal radius of 30 pc and the red diamonds represent the Lagrangian radii for a fractal radius of 50 pc.

Acknowledgements: CA, FUZ and AAJ acknowledge funding through Fondecyt Regular No. 1180291 and the Chilean BASAL Centro de Excelencia en Astrofisica y Tecnologias Afines (CATA) grant PFB-06/2007. MF acknowledges support through Fondecyt regular 1180291, Basal AFB-170002 and PII20150171.

References

Alarcón Jara A.G., et al., 2018, MNRAS, 473, 5015
Assmann P., et al., 2013a, MNRAS, 432, 274
Assmann P., et al., 2013b, MNRAS, 435, 2391
Domínguez R., et al., 2017, MNRAS, 472, 465
D'Onghia E., et al., 2009, Nature, 460, 605
Goodwin S.P., Whitworth A.P., 2004, A&A, 413, 929
Mayer L., et al., 2007, Nature, 445, 738
Metz M., Kroupa P., Jerjen H., 2007, MNRAS, 374, 1125
Okamoto S., et al., 2012, ApJ, 744, 96
Plummer H.C., 1911, MNRAS, 71, 460
Tollerud E.J., et al., 2011, ApJ, 726, 108
Vincenzo F., et al., 2014, MNRAS, 441, 2815